ELSEVIER

Oilwell Cement Clinkers

X-ray Microanalysis and Phase Composition

Christopher Hall and Karen L. Scrivener*
Schlumberger Cambridge Research, High Cross, Cambridge, United Kingdom; and Department of Materials, Imperial College, London, United Kingdom

*X-ray microanalyses have been made on a suite of nine oilwell cement clinkers. Elemental data were obtained on alite, belite, and ferrite phases and, for two clinkers only, also on aluminate. The alite and belite compositions are broadly similar to those previously reported for other portland cements. Guest ion concentrations suggest that several charge-balancing substitutions occur. Bulk MgO and SO_3 levels determine the Mg and S contents of both phases, but for Fe and Al the substitution levels are not strongly correlated with bulk composition. For ferrites, the data are generally consistent with the results of Bergstrom et al. (*Adv Cem Res **1992,** 4, *141–147): the Mg content varies widely, is controlled by the bulk MgO, and is coupled with Si in a charge-balancing substitution for Fe. Estimates of the total phase assembly using the directly determined mineral compositions are compared with the predictions of a modified Bogue calculation (similar to that of Taylor,* Adv Cem Res **1989,** 2, *73–77). The agreement is variable and some refinements to the method of calculation are indicated.* Advanced Cement Based Materials 1998, 7, 28–38. © *1998 Elsevier Science Ltd.*

KEY WORDS: Cement, Clinker, Microanalysis, Alite, Belite, Ferrite

Many X-ray microanalyses of cement clinkers have been published previously [1–7] but few of these are for oilwell cement materials. In an earlier paper [8] we reported the results of an X-ray microanalysis of the interstitial material in a suite of eight oilwell cement production clinkers. We have now extended this work to the silicate phases. The materials included in the later study that is described here comprised five of the original suite and four additional clinkers. New analytical data were also obtained on the interstitial material. For these nine clinkers, a fuller statistical analysis is now possible.

Address correspondence to: C. Hall, Schlumberger Cambridge Research, High Cross, Madingley Road, Cambridge CB3 0EL, United Kingdom.
Received January 20, 1997; Accepted March 17, 1997
*Present address: Lafarge, Laboratoire central de recherche, 95 rue du Montmurier BP 15, 38291 Saint-Quentin-Fallavier, France.

Experimental

The materials used were drawn from primary samples (typically 1 to 5 kg) of production clinkers. They were supplied from a number of plants in several countries. The suite was chosen to represent a typical range of clinkers for API class G or class H oilwell cements. We denote the individual materials D1 through D9. D1 to D5 were taken from the same batches as materials for which ferrite data were reported in our earlier paper [8] (see footnote, Table 1).

Bulk chemical analyses were carried out by standard X-ray fluorescence (XRF) methods (major and minor oxides) and by wet methods for free lime and SO_3. The results are given in Table 1.

Specimens for microanalysis were prepared as described previously [8]. A sub-sample of several tens of grams of each clinker was crushed and homogenized. Material from the 1 to 4 mm size fraction was mounted in epoxy resin and polished to 1/4 μm. X-ray microanalyses were made by energy-dispersive spectroscopy (EDS). Quantitative estimates of elemental composition were obtained by comparison with stored standard spectra and using the ZAF procedure. For each clinker at least 10 EDS analyses were made for each phase. For a given phase, each analysis was made on a different piece of clinker. In total, approximately 500 spot analyses were obtained. In addition, X-ray diffraction (XRD) powder patterns and scanning electron microscopy (SEM) back-scattered electron images were recorded.

For these anhydrous phases, at the accelerating voltage of 15 kV used, each microanalysis relates to a volume somewhat less than 1 μm in each dimension. All analyses were taken well away from phase boundaries, as far as could be judged from the two-dimensional section. For alite and belite, analytical errors attributed to X-rays coming from adjacent phases (which may in some cases be beneath the plane of the section and thus invisible) is not considered a significant source of error. In the case of the other phases (the ferrite and particularly the aluminate, where identified), the risk of contamination is greater. Interstitial ferrite is irregular and aluminate has

ISSN 1065-7355/98/$19.00
PII S1065-7355(97)00035-7

TABLE 1. Oxide analysis for clinkers

	D1	D2	D3	D4	D5	D6	D7	D8	D9
Na_2O	0.11	0.11	0.09	0.19	0.08	0.21	0.09	0.08	0.14
MgO	2.33	0.80	0.70	0.90	1.80	1.65	1.90	0.75	0.70
Al_2O_3	3.98	3.40	3.55	4.80	3.30	3.70	3.40	3.70	3.75
SiO_2	21.68	22.60	22.95	21.65	22.95	22.40	23.20	22.00	23.60
SO_3	1.15	1.10	1.02	0.17	0.60	0.81	0.52	0.20	0.20
P_2O_5	0.21	0.00	0.00	0.21	0.13	0.04	0.13	0.11	0.11
K_2O	0.54	0.54	0.41	0.17	0.54	0.55	0.48	0.47	0.67
CaO	64.86	66.20	66.20	65.75	65.15	65.05	64.95	65.30	64.90
TiO_2	0.30	0.0	0.16	0.24	0.18	0.19	0.17	0.16	0.17
Mn_2O_3	0.03	0.0	0.07	0.06	0.16	0.06	0.15	0.19	0.17
Fe_2O_3	4.66	5.20	4.25	5.10	4.55	4.95	4.65	6.75	4.65
loss	0.00	0.20	0.15	0.50	0.40	0.35	0.20	0.45	0.30
residue	0.13	0.0	0.01	0.09	0.15	0.02	0.08	0.11	0.02
Free lime	0.90	0.60	0.25	0.55	0.60	0.25	0.35	0.55	0.40
Total	99.85	100.15	99.55	99.74	99.84	99.96	99.84	100.16	99.36

Note: Samples D1, D2, D3, D4, and D5 are taken from the same batches as samples C5, C9, C7, C3, and C6, respectively, of Bergstrom et al. [8].

small grain size, usually around 1 μm or less. Spot analyses that departed dramatically from stoichiometry (>10%) were discarded as being unreliable. Even so, the results for the aluminate phase should still be treated with some caution.

It is difficult to give a precise value for the accuracy of EDS microanalysis. The microscope employed in this study is used exclusively for the examination of cementitious materials and the accuracy of the standards correction has been optimized for these materials. We consider that the accuracy of individual element spot analyses probably approaches 0.1 atom or weight % (1 part in 10^3). However, when several analyses are made on a phase, the observed compositional variations from point to point are much greater than this, so that measurement errors contribute relatively little to the statistical variance. Consideration of charge balance and stoichiometry suggest that the overall accuracy of the mean values from each phase were perhaps better than 0.1%, so that values are quoted to 0.01%.

Silicate Phases

Composition

In Tables 2 and 3 we show the compositions of alite and belite phases in the suite of clinkers examined. These are the means of the individual spot analyses for each clinker. Variances are also tabulated. Taken as a whole these compositions (both means and ranges) are similar to those previously reported for construction cements [1–7]. However, the alite Fe in these Fe-rich clinkers is rather higher, as is the Al, in spite of the low bulk Al. In the belite, the sulphate content is notably higher than reported elsewhere. In both silicate phases the Mg is, as usual, very variable from clinker to clinker, but there is much less variation in Al and Fe contents. In these clinkers, between one quarter and one third of the total Al resides in the silicate phases. Overall minor oxide levels are in the range of 2.7 to 4.4 wt % for alite and 3.6 to 6.2 wt % for belite.

Variation in Composition Within Clinkers

The spread of local compositions as sampled by individual spot analyses is a measure (albeit a rough one) of the structural homogeneity of the phase. For both alite and belite phases the compositions are quite erratic, as can be seen from the variances of the main minor oxides such as MgO, Al_2O_3, and Fe_2O_3 (see also the cluster plots of Figure 1). These variances are generally smaller than those of the minor oxides of the ferrite phase.

Guest Ions and Substitution Patterns

Statistical analysis of the individual spot compositions reveals several internal correlations between the concentrations of certain elements in the composition data set. We have calculated the correlation matrix for the entire alite spot analysis dataset, and likewise for the belite dataset. The more significant correlation coefficients ($r > 0.5$) are given in Table 4. For alite, we find strong inverse correlations between Mg and Ca and between Al and Si; and a positive correlation between Al and Fe.

For belite, there is a similar strong inverse correlation between Al and Si, and a positive correlation between Al and Fe. There is also a clear inverse correlation between Si and S.

The correlations reflect the complexities of the underlying substitution patterns in these calcium silicate minerals. To help more detailed discussion, we express the composition in terms of the parent structural formula units: for alite, Ca_3SiO_5, normalizing the atomic

TABLE 2. Alite oxide compositions in the clinker suite

	D1	D2	D3	D4	D5	D6	D7	D8	D9	Mean
Na_2O	0.01	0.0	0.08	0.04	0.0	0.05	0.0	0.0	0.07	0.01
	0.29	0.30	0.23	0.27	0.29	0.12	0.18	0.25	0.26	0.25
MgO	1.19	0.23	0.29	0.19	1.13	0.87	1.07	0.30	0.28	0.62
	0.33	0.28	0.23	0.22	0.40	0.23	0.20	0.27	0.29	0.49
Al_2O_3	1.47	1.25	1.10	1.07	1.20	1.30	1.14	1.32	1.29	1.25
	0.40	0.29	0.39	0.38	0.42	0.38	0.36	0.32	0.59	0.41
SiO_2	24.56	24.92	24.73	25.99	25.18	25.30	25.09	24.80	25.05	25.06
	0.52	0.63	0.57	0.56	0.69	0.88	0.47	0.50	0.93	0.76
SO_3	0.38	0.46	0.30	0.25	0.11	0.35	0.12	0.17	0.12	0.24
	0.22	0.18	0.26	0.22	0.17	0.30	0.15	0.18	0.21	0.24
Cl	0.04	0.07	0.02	0.09	0.08	0.0	0.04	0.0	0.04	0.03
	0.07	0.06	0.10	0.09	0.10	0.09	0.08	0.10	0.07	0.09
K_2O	0.06	0.04	0.09	0.03	0.07	0.13	0.03	0.14	0.15	0.09
	0.11	0.10	0.10	0.08	0.05	0.13	0.13	0.13	0.10	0.11
CaO	71.07	71.50	72.43	71.33	71.21	70.70	71.37	72.15	71.37	71.46
	0.90	0.46	0.74	0.63	0.80	0.79	0.71	0.57	0.84	0.88
TiO_2	0.0	0.0	0.0	0.0	0.0	0.0	0.0	0.0	0.0	0.0
	0.15	0.18	0.24	0.20	0.14	0.17	0.20	0.14	0.21	0.19
Mn_2O_3	0.08	0.20	0.07	0.06	0.07	0.12	0.12	0.17	0.18	0.10
	0.21	0.18	0.26	0.27	0.21	0.24	0.25	0.24	0.20	0.24
Fe_2O_3	1.13	1.44	1.09	0.98	1.04	1.12	1.12	1.00	1.52	1.18
	0.45	0.36	0.40	0.39	0.41	0.52	0.45	0.21	0.58	0.46

Notes: For each element, the mean and standard deviation of the X-ray spot analyses are expressed as oxide and normalized to 100 mass percent; the last column gives standard deviations for each element for the entire dataset, not means of the standard deviations for each clinker.

composition to 5 O atoms; and for belite, Ca_2SiO_4, normalizing the atomic composition to 4 O atoms. This is shown in Tables 5 and 6.

ION SUBSTITUTION IN ALITE. The observed inverse correlation between Ca and Mg in alite is consistent with the isomorphous divalent substitution $MgCa_{-1}$. Recent nuclear magnetic resonance (NMR) data [9] indicates that Al substitutes almost exclusively in tetrahedral Si sites in a synthetic alite and various clinkers. This substitution requires charge balancing. For the solid solution C_3S–Al_2O_3, Midgley and Fletcher [10] proposed the

TABLE 3. Belite oxide compositions

	D1	D2	D3	D4	D5	D6	D7	D8	D9	Mean
Na_2O	0.10	0.08	0.11	0.25	0.17	0.19	0.07	0.05	0.10	0.12
	0.19	0.22	0.31	0.25	0.19	0.21	0.31	0.29	0.17	0.25
MgO	0.06	0.0	0.0	0.0	0.09	0.14	0.17	0.0	0.0	0.0
	0.28	0.21	0.21	0.22	0.37	0.28	0.29	0.31	0.28	0.30
Al_2O_3	1.75	1.56	1.63	1.69	1.35	1.84	1.64	1.36	1.06	1.55
	0.30	0.21	0.23	0.34	0.22	0.29	0.38	0.50	0.37	0.41
SiO_2	30.69	31.44	30.92	32.09	31.59	31.28	31.52	32.25	32.77	31.64
	0.60	0.97	0.60	0.79	0.24	0.75	0.75	1.21	1.06	1.05
SO_3	1.69	1.38	1.28	0.73	0.58	1.48	0.88	0.49	0.31	0.97
	0.38	0.31	0.48	0.43	0.16	0.98	0.31	0.44	0.22	0.67
Cl	0.01	0.05	0.04	0.06	0.04	0.01	0.02	0.00	0.03	0.03
	0.07	0.07	0.09	0.12	0.04	0.11	0.10	0.08	0.09	0.09
K_2O	0.39	0.37	0.59	0.46	0.41	0.64	0.47	0.58	0.77	0.54
	0.23	0.12	0.31	0.22	0.12	0.39	0.14	0.23	0.27	0.28
CaO	63.55	63.54	63.65	63.42	64.16	62.49	63.38	63.93	63.61	63.49
	0.64	0.27	0.95	0.77	0.73	0.74	0.84	0.92	0.76	0.86
TiO_2	0.18	0.0	0.01	0.0	0.00	0.0	0.04	0.0	0.0	0.01
	0.19	0.20	0.22	0.21	0.15	0.19	0.14	0.10	0.18	0.19
Mn_2O_3	0.02	0.0	0.14	0.02	0.0	0.03	0.09	0.17	0.09	0.07
	0.20	0.24	0.20	0.25	0.13	0.20	0.16	0.20	0.21	0.21
Fe_2O_3	1.55	1.82	1.71	1.43	1.60	1.93	1.72	1.44	1.55	1.63
	0.32	0.46	0.39	0.33	0.40	0.56	0.46	0.60	0.65	0.50

Notes: For each element, the mean and standard deviation of the X-ray spot analyses are expressed as oxide and normalized to 100 mass percent; the last column gives standard deviations for each element for the entire dataset, not means of the standard deviations for each clinker.

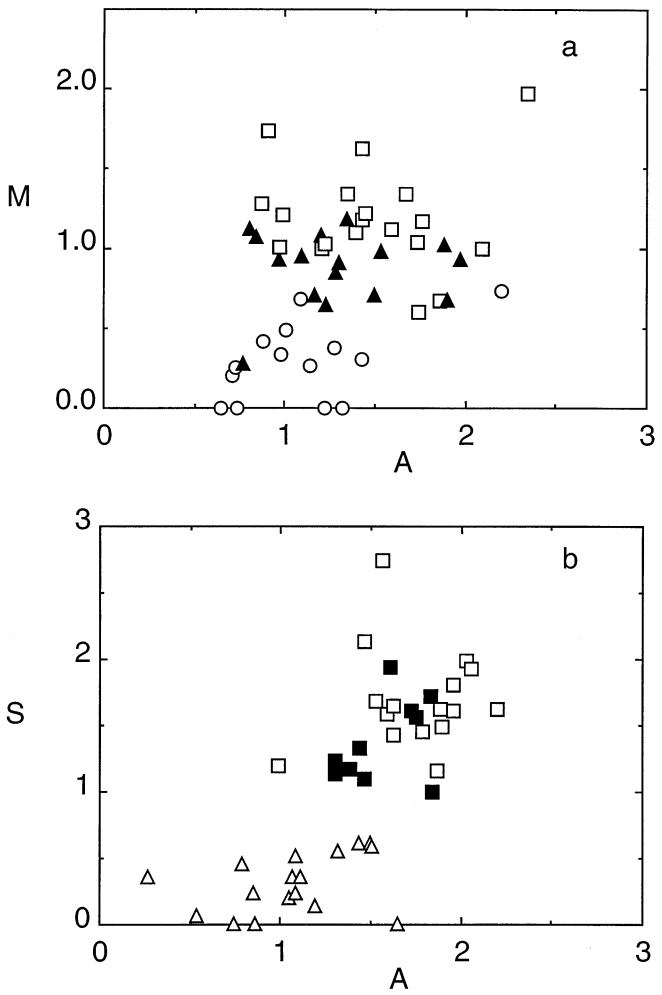

FIGURE 1. Cluster plots showing typical variation of some minor oxide concentrations in alite and belite spot analyses. (a) MgO and Al_2O_3 in alite (clinkers D1 □, D3 ○, and D6 ▲ only are included for clarity); (b) SO_3 and Al_2O_3 in belite (clinkers D1 □, D2 ■, and D9 △).

simple substitution $4Al(3Si)_{-1}$, with excess Al occupying a vacant lattice site. Hahn et al. [11] argued also for the substitution $FeCa_{-1}$ in the system C_3S–Fe_2O_3. The positive correlation between Fe and Al and the inverse correlation between Ca and Fe concentrations in our clinker alites suggest (for these Fe-rich production clinkers at least) that the substitution $FeCa_{-1}$ may provide one mechanism for charge compensation. In any case, in production clinkers such as these with numerous guest ions, several other contributions to overall charge balance can easily be envisaged. These cannot be discerned from microanalytical data alone. Therefore, we employ the conventional cation sums (Ca + Mg + K + Na + Fe + Mn) and (Al + Si + S + Ti), which are shown in Table 5. For these clinkers, these sums vary somewhat both above and below the stoichiometric values of the parent tricalcium silicate. The charge sums

TABLE 4. Correlation coefficients expressing the more significant correlations between the concentrations of individual elements in the clinker phases

Phase	Correlation Coefficient
Alite (n = 142)	
Mg, Ca	−0.57
Al, Si	−0.70
Al, Fe	+0.62
Si, Fe	−0.52
Belite (n = 136)	
Al, Si	−0.72
Al, Fe	+0.54
Si, S	−0.68
Ferrite (n = 173)	
Mg, Fe	−0.61
Si, Fe	−0.63

Included are all Pearson product-moment correlation coefficients >0.5 (highly significant); n is the sample size.

for the cations and the framework elements are also included in Table 5. The simplest explanatory model consistent with the microanalytical data is that Al and S substitute for Si and this substitution is charge-balanced by a combination of Fe, Na, K, and Mn substituted for Ca. The alite S levels in these clinkers are always low (<0.5 wt %) and the SO_4 ion does not appear to play an important part in the alite substitution chemistry.

ION SUBSTITUTION IN BELITE. In belite (in contrast to alite) S does have an important role in the substitution patterns. It is known that SO_3 is concentrated in the belite phase but the levels found here are very variable and frequently high (range 0.3 to 1.7 wt %) [12]. Statistically significant inverse correlations are found between the concentrations of Si and Al (−0.72) and between Si and S (−0.68). In most clinkers Al and Fe spot concentrations are also positively correlated, although the overall correlation coefficient for the entire suite is only 0.54. The cation charge subtotals are given in Table 6. They behave much as the alite totals do, except that the Si + Al + S charge never exceeds 4.0, even though the S levels are invariably quite high. Recently obtained NMR data [9] show that Al substitutes exclusively for Si in a synthetic substituted dicalcium silicate. The present data therefore support a charge-balancing substitution involving S/Al for Si. However, considerable Fe is also present in these belites. The location of the Fe must remain an open question but the overall charge-balance is found to be closer to the C_2S parent if Fe is partitioned equally between the Ca-type and tetrahedral (Si-type) sites. There is also a weak inverse correlation (−0.41) between the belite Ca and Fe spot concentrations. Both features suggest some substitution of Fe into Ca sites.

TABLE 5. Mean molar compositions of alite phase, atoms per five oxygen atoms

	D1	D2	D3	D4	D5	D6	D7	D8	D9	Mean
Na	0.001	0.0	0.006	0.003	0.0	0.004	0.0	0.0	0.005	0.001
Mg	0.067	0.013	0.016	0.011	0.064	0.049	0.061	0.017	0.016	0.035
Al	0.066	0.056	0.049	0.048	0.054	0.058	0.051	0.059	0.058	0.055
Si	0.932	0.947	0.942	0.982	0.953	0.956	0.952	0.944	0.954	0.951
S	0.011	0.013	0.008	0.007	0.003	0.010	0.003	0.005	0.003	0.007
Cl	0.002	0.004	0.001	0.005	0.004	0.0	0.002	0.0	0.002	0.002
K	0.003	0.002	0.004	0.002	0.003	0.006	0.002	0.007	0.007	0.004
Ca	2.890	2.911	2.956	2.887	2.890	2.864	2.904	2.944	2.913	2.906
Ti	0.0	0.0	0.0	0.0	0.0	0.0	0.0	0.0	0.0	0.0
Mn	0.002	0.006	0.002	0.002	0.002	0.0	0.003	0.004	0.005	0.002
Fe	0.032	0.041	0.031	0.028	0.030	0.040	0.032	0.029	0.043	0.034
cation	3.00*	2.97	3.02	2.93	2.98	2.96	3.00	3.00	2.99	2.98
subtotals	1.01†	1.01	0.99	1.04	1.01	1.02	1.01	1.01	1.01	1.01
charge	6.02*	5.99	6.06	5.89	6.00	5.95	6.03	6.03	6.01	6.00
subtotals	3.99†	4.03	3.94	4.11	3.99	4.05	3.98	3.98	4.00	4.01

Total cation charge is calculated assuming formal charges: Fe, Mn +3; S +6.
*Na + Mg + K + Ca + Mn + Fe.
†Al + Si + S + Ti.

Distribution of Minor Oxides Between Alite and Belite

Figure 2 shows the partitioning of the minor oxides in alite and belite phases in the same clinker. K and S are strongly concentrated in the belite; Mg is concentrated somewhat in the alite. Na levels are too low for definite conclusions, although this element appears to associate with K. Al and Fe are not strongly selected, although Fe has a weak preference for belite. These observations agree qualitatively with those of Ghose and Barnes [5a, 5b] and Kristmann [6].

Interstitial Material

The new microanalytical data on the interstitial material confirm to a large extent the previously published results [8]. The overall picture is of highly variable interstitial compositions, with large clinker-to-clinker variance and substantial textural variation within individual clinker nodules. This is also consistent with the observations of Richardson et al. [13], who showed on a single clinker specimen that composition swings equal to the entire sample range occurred over traverses of a few microns.

In Table 7, we give the oxide compositions of the ferrite phase in each clinker; in Table 8 the compositions are expressed as atoms per 10 oxygen atoms.

In these Fe-rich oilwell clinkers, aluminate is either absent or rare. However, in two cases (D4 and D8), aluminate material was identified in the back-scattered electron image in sufficient amount to allow X-ray microanalysis. Aluminate compositions for D4 and D8

TABLE 6. Mean molar compositions of belite phase, atoms per four oxygen atoms

	D1	D2	D3	D4	D5	D6	D7	D8	D9	Mean
Na	0.005	0.004	0.006	0.014	0.010	0.011	0.004	0.003	0.006	0.007
Mg	0.003	0.0	0.0	0.0	0.004	0.006	0.007	0.0	0.0	0.0
Al	0.059	0.053	0.056	0.058	0.046	0.062	0.056	0.046	0.036	0.053
Si	0.884	0.905	0.895	0.924	0.914	0.901	0.911	0.933	0.947	0.913
S	0.037	0.030	0.028	0.016	0.013	0.032	0.019	0.011	0.007	0.021
Cl	0.001	0.002	0.002	0.002	0.002	0.000	0.001	0.0	0.001	0.001
K	0.014	0.013	0.022	0.017	0.015	0.023	0.017	0.021	0.028	0.019
Ca	1.962	1.960	1.974	1.957	1.989	1.928	1.962	1.978	1.971	1.965
Ti	0.004	0.0	0.0	0.0	0.0	0.0	0.001	0.0	0.0	0.0
Mn	0.001	0.0	0.003	0.0	0.0	0.001	0.002	0.004	0.002	0.001
Fe	0.034	0.040	0.037	0.031	0.035	0.042	0.037	0.031	0.034	0.036
cation	2.02*	2.01	2.04	2.01	2.05	2.01	2.03	2.03	2.03	2.03
subtotals	0.98†	0.99	0.98	1.00	0.97	0.99	0.99	0.99	0.99	0.99
charge	4.07*	4.04	4.09	4.03	4.12	4.03	4.08	4.07	4.06	4.06
subtotals	3.93†	3.96	3.91	3.96	3.87	3.98	3.93	3.93	3.94	3.94

Total cation charge is calculated assuming formal charges: Fe, Mn +3; S +6.
*Na + Mg + K + Ca + Ti + Mn + Fe.
†Al + Si + S.

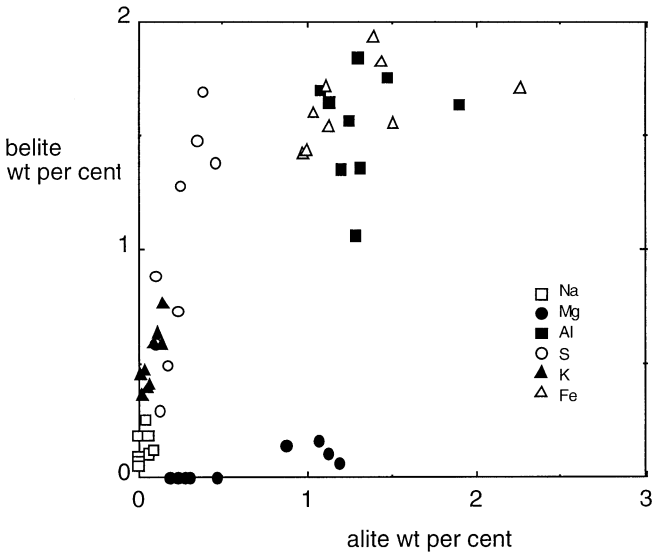

FIGURE 2. Distribution of minor oxides between alite and belite phases.

are given in Table 9, expressed as oxides and in Table 10 as atoms per formula unit related to the parent structure $Ca_3Al_2O_6$.

Guest Ions in Ferrites

Substitution patterns in Fe-rich portland cement interstitial material were discussed in detail by Bergstrom et al. [8]. The dominant feature is the substitution of Mg for Fe, with charge balancing by coupled substitution of Si, Ti for further Fe: that is, $2FeMg_{-1}(Si,Ti)_{-1}$. Richardson et al. [13] suggested that Mn (as a divalent cation) also may substitute for Fe (Mn levels are generally very small). There was no strong evidence for isomorphous substitution of Mg for Ca. In our previous paper [8], we showed that the molar quantities A_m and F_m^{eq} fall compactly on the join between the corresponding Taylor ferrite compositions [14]. (A_m is $\frac{1}{2}$ Al_2O_3 expressed as mol/100 g clinker; F_m^{eq} is the sum of the amounts of $\frac{1}{2}$ Fe_2O_3, MgO, SiO_2, TiO_2 and $\frac{1}{2}$ Mn_2O_3, also expressed as mol/100 g clinker.) For comparison with earlier data, Figure 3 shows a plot of A_m versus F_m^{eq}. The tendency noted previously for compositions to extend to higher Fe contents than that represented by Taylor's low Al ferrite is more pronounced in this dataset. This suggests that for oilwell cement compositions the low Al ferrite (the effective end member of the ferrite solid solution series) may be somewhere around $Ca_2Al_{0.65}Fe_{1.35}O_5$. We have also calculated from the spot analyses the indices x, which describes the extent of the substitution 2Fe Mg_{-1} (Si, Ti)$_{-1}$, and A_m/F_m^{eq}, which is the generalized A/F ratio of the ferrite. The mean values for each clinker are given in Table 11. The anomalous value previously reported [8] for D4 can now be attributed to the contribution of C_3A to a few spot analyses.

Guest Ions in Aluminates

The crystal structure refinements of Takéuchi et al. [15] have established the main substitution patterns in C_3A.

TABLE 7. Ferrite oxide compositions

	D1	D2	D3	D4	D5	D6	D7	D8	D9	Mean
Na_2O	0.06	0.01	0.17	0.17	0.0	0.17	0.05	0.0	0.07	0.06
	0.24	0.21	0.29	0.25	0.28	0.34	0.27	0.21	0.25	0.27
MgO	5.19	2.29	2.59	2.52	4.12	4.65	4.86	1.93	1.62	3.29
	0.84	0.35	0.34	0.21	0.77	1.24	1.25	0.37	0.41	1.51
Al_2O_3	16.08	14.11	14.53	18.51	14.62	16.91	15.00	16.98	14.40	15.66
	1.04	1.62	1.67	1.44	1.29	1.18	1.59	2.49	2.91	2.25
SiO_2	5.75	3.80	5.15	5.17	5.68	5.49	5.83	4.05	3.42	4.90
	0.47	0.60	0.64	1.08	0.59	0.76	1.68	2.36	2.22	1.62
SO_3	0.90	0.36	0.35	0.20	0.14	0.18	0.13	0.08	0.06	0.29
	0.49	0.26	0.21	0.12	0.24	0.33	0.18	0.22	0.21	0.38
Cl	0.04	0.01	0.03	0.07	0.05	0.07	0.03	0.03	0.03	0.03
	0.10	0.11	0.10	0.08	0.12	0.11	0.09	0.09	0.07	0.10
K_2O	0.18	0.11	0.13	0.13	0.06	0.17	0.21	0.07	0.26	0.15
	0.19	0.16	0.13	0.14	0.07	0.13	0.16	0.10	0.44	0.20
CaO	47.92	46.34	47.84	48.14	47.77	47.34	47.90	47.74	46.26	47.49
	0.69	0.63	1.20	1.24	0.82	0.73	1.36	1.36	1.48	1.27
TiO_2	0.79	0.49	0.40	0.69	0.55	0.34	0.30	0.49	0.35	0.50
	0.18	0.18	0.20	0.36	0.24	0.20	0.28	0.25	0.26	0.29
Mn_2O_3	0.21	0.59	0.63	0.34	0.96	0.29	0.65	1.34	0.83	0.67
	0.20	0.30	0.30	0.27	0.29	0.24	0.46	0.55	0.60	0.52
Fe_2O_3	22.88	31.90	28.17	24.06	26.12	24.38	25.04	27.35	32.68	26.95
	0.92	1.09	1.94	2.62	1.26	1.66	2.97	2.30	4.11	3.97

Notes: For each element, the mean and standard deviation of the X-ray spot analyses are expressed as oxide and normalized to 100 mass percent; the last column gives standard deviations for each element for the entire dataset, not means of the standard deviations for each clinker.

TABLE 8. Mean molar compositions of ferrites, atoms per 10 oxygen atoms

	D1	D2	D3	D4	D5	D6	D7	D8	D9	Mean
Na	0.001	0.001	0.027	0.036	0.0	0.026	0.008	0.0	0.011	0.010
Mg	0.602	0.276	0.309	0.295	0.488	0.543	0.573	0.230	0.197	0.390
Al	1.475	1.344	1.368	1.709	1.368	1.563	1.398	1.601	1.381	1.468
Si	0.447	0.307	0.412	0.404	0.451	0.431	0.460	0.323	0.277	0.390
S	0.052	0.022	0.021	0.012	0.008	0.011	0.007	0.005	0.004	0.016
Cl	0.004	0.001	0.003	0.008	0.005	0.007	0.007	0.005	0.004	0.004
K	0.018	0.011	0.013	0.013	0.006	0.017	0.021	0.007	0.027	0.015
Ca	3.997	4.017	4.099	4.043	4.065	3.978	4.059	4.093	4.041	4.044
Ti	0.046	0.030	0.024	0.041	0.033	0.020	0.018	0.029	0.022	0.029
Mn	0.012	0.037	0.038	0.020	0.058	0.017	0.039	0.082	0.052	0.040
Fe	1.341	1.943	1.696	1.421	1.562	1.440	1.492	1.648	2.010	1.617
Cation	4.03*	4.03	4.14	4.08	4.06	4.02	4.09	4.09	4.08	4.07
Subtotals	3.98†	3.96	3.87	3.90	3.97	4.02	3.99	3.92	3.94	3.95
Charge	8.02*	8.05	8.24	8.13	8.12	8.00	8.15	8.18	8.12	8.11
Subtotals	11.98†	12.00	11.80	11.89	11.93	12.01	11.89	11.89	11.94	11.93

Total cation charge is calculated assuming formal charges: Fe, Mn +3; S +6.
*Na + K + Ca.
†Mg + Al + Si + S + Ti + Mn + Fe.

The more important of these are the simple charge-conserving replacements of $MgCa_{-1}$ in octahedral sites and $FeAl_{-1}$ in tetrahedral sites on the Al_6O_{18} rings; and the coupled charge-balancing substitutions $(Na, K)_2Ca_{-1}\square_{-1}$, where $\square$ denotes a normally vacant site at the center of the ring; and $AlSi_{-1}Ca_{-1}(Na, K)_{-1}$. The microanalytical data of Han et al. [16] on multicomponent synthetic aluminates are consistent with Takéuchi's crystallographic conclusions. In production clinkers all of these substitutions may contribute to the observed solid solution. However, the requirement of overall charge balance must be satisfied. Our microanalytical data are rather sparse since aluminate was identified in only two of these clinkers, but they agree for the most part with analyses reported elsewhere [2,7,17]. The principal guest ions are Fe and Si, with lesser amounts of Mg, Na, and K. Approximately one in eight of the tetrahedral sites is occupied by Fe and an equal number by Si. Kristmann [6] found similar high levels of Fe but our Si concentrations are greater than reported elsewhere. The amounts of Si are much higher than the amounts of Na + K, so that excess Si charge could be balanced by a Ca deficit [2]. How-

TABLE 9. Aluminate oxide compositions

	D4	D8
Na_2O	1.58	0.46
	0.54	0.33
MgO	1.47	1.12
	0.43	0.86
Al_2O_3	27.75	29.00
	2.14	1.06
SiO_2	5.57	4.97
	0.98	1.37
SO_3	0.18	0.20
	0.27	0.26
Cl	0.04	0.04
	0.11	0.10
K_2O	0.74	1.34
	0.24	1.29
CaO	55.29	56.94
	1.56	2.83
TiO_2	0.0	0.0
	0.23	0.13
Mn_2O_3	0.04	0.13
	0.17	0.26
Fe_2O_3	7.45	5.95
	2.91	2.35

Notes. For each element, the mean and standard deviation of the X-ray spot analyses are expressed as oxide and normalized to 100 mass percent; the last column gives standard deviations for each element for the entire dataset, not means of the standard deviations for each clinker.

TABLE 10. Mean molar composition of the aluminate phase, atoms per six oxygen atoms

	D4	D8	Mean
Na	0.139	0.040	0.090
Mg	0.099	0.076	0.088
Al	1.482	1.550	1.516
Si	0.253	0.225	0.239
S	0.006	0.007	0.006
Cl	0.003	0.002	0.003
K	0.043	0.078	0.060
Ca	2.685	2.767	2.725
Ti	0.0	0.0	0.0
Mn	0.002	0.004	0.003
Fe	0.255	0.203	0.229
cation	2.97*	2.96	2.97
subtotals	1.99†	1.98	1.99
charge	5.76*	5.82	5.79
subtotals	6.24†	6.18	6.21

Total cation charge is calculated assuming formal charges: Fe, Mn +3; S +6.
*Na + Mg + K + Ca + Mn.
†Al + Si + S + Ti + Fe.

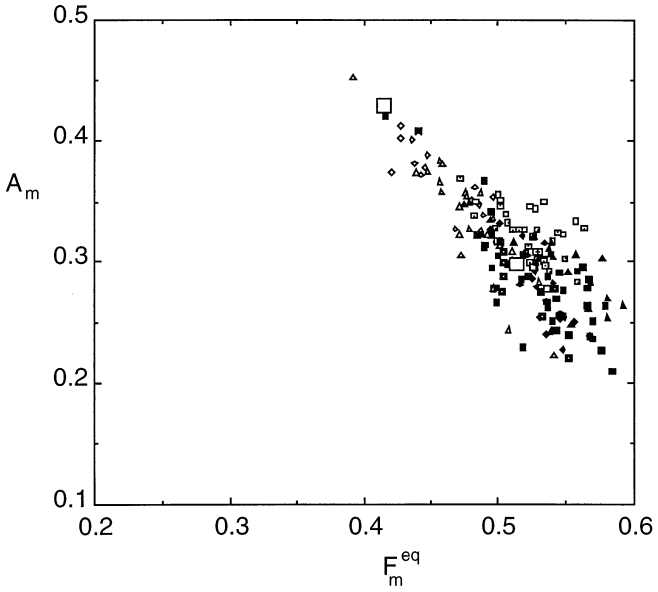

FIGURE 3. A_m vs F_m^{eq}, ferrites (spot analyses of all clinkers). Large open squares mark the Taylor ferrite compositions.

ever, the charges calculated on that basis do not balance (Table 10). It is possible that there may be a contribution from divalent Fe incorporated into Ca-type sites. This remains an open question. We have also noted earlier that the aluminate microanalyses may be subject to some errors arising from contamination by other phases.

Relation Between Bulk Composition and Composition of Individual Phases

We tested the data for correlations between the mean compositions of individual phases and the bulk composition for all clinkers and all elements. There are several strong, statistically significant, positive correlations. These are valuable in providing empirical rules for estimating phase compositions when bulk data only are available. The significant correlations are summarized in Table 12. In calculating these correlations, the raw bulk oxide data have been corrected for free lime and soluble sulphates. The measured free lime has been subtracted from the total CaO. The soluble sulphates present have been computed according to the rules given by Taylor [14] and the SO_3 equivalent to these soluble sulphates has been subtracted from the total SO_3 given by bulk oxide analysis in Table 1. The sum of the oxides is then normalized to 1.00.

TABLE 11. Composition indices A_m/F_m^{eq} and x for ferrite phase

	A_m/F_m^{eq}	x
D1	0.60	0.226
D2	0.52	0.125
D3	0.56	0.158
D4	0.79	0.175
D5	0.53	0.198
D6	0.64	0.205
D7	0.55	0.211
D8	0.70	0.143
D9	0.55	0.108

$A_m/F_m^{eq} = \frac{1}{2}Al_2O_3/(\frac{1}{2}Fe_2O_3 + MgO + SiO_2 + TiO_2 + \frac{1}{2}Mn_2O_3)$ and $x = a/[2(1 + a)]$, where $a = (MgO + SiO_2 + TiO_2 + \frac{1}{2}Mn_2O_3)/\frac{1}{2}Fe_2O_3$ with all quantities expressed as mol/100 g clinker.

TABLE 12. The more significant correlations between elemental compositions of individual phases and bulk compositions (linear correlation coefficients)

	Alite	Belite	Ferrite
Mg	0.97	0.72	0.96
Al	ns	ns	0.83
Si	ns	ns	ns
S total	0.76	0.91	0.74
S corrected*	0.85	0.95	0.81
K	0.65	ns	ns
Fe	0.72	ns	ns

ns = not highly significant (<0.6).
*S corrected for soluble sulphates (see text).
Summary of regression equations for elements and minerals with r >0.8 (all wt %):
MgO(alite) = 0.64MgO(bulk) − 0.23
MgO(ferrite) = 2.0MgO(bulk) + 0.64
Al_2O_3(ferrite) = 2.8Al_2O_3(bulk) + 5.0
SO_3(belite) = 1.23SO_3(bulk, total) + 0.24
SO_3(alite) = 0.72SO_3(bulk, corrected) + 0.15
SO_3(belite) = 3.36SO_3(bulk, corrected) + 0.55
SO_3(ferrite) = 1.43SO_3(bulk, corrected) + 0.10.

Alite

There is strong positive correlation between alite Mg and bulk MgO, and somewhat weaker ones for S, Fe, and K. For Mg, we find

$$\text{wt \% } MgO\ (alite) = 0.64\ MgO\ (bulk) - 0.23$$

which may be compared with Taylor's equation [14] $MgO = 0.667\ MgO\ (bulk)$, up to a maximum of 2 wt %. Maki et al. [18] find $MgO = 0.58\ MgO\ (bulk)$.

We find that the alite S, while low, is significantly correlated with the bulk SO_3 corrected for soluble sulphates and also with the total bulk SO_3 (see Table 12). Thus,

$$\text{wt \% } SO_3\ (alite) = 0.72\ SO_3\ (bulk, corrected\ for\ estimated\ soluble\ sulphates) + 0.15.$$

It is known that high bulk clinker SO_3 encourages the formation of the alite M_1 polymorph and so this correlation may have some predictive value [1].

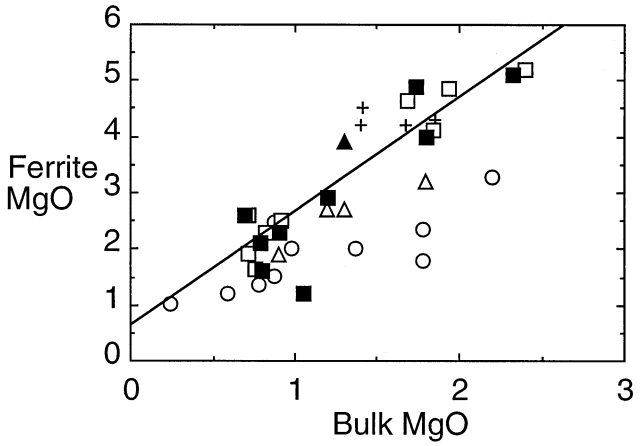

FIGURE 4. MgO (ferrite) vs MgO (bulk). Symbols: ○ Ghose and Barnes [5a, 5b]; ■ Bergstrom et al. [8]; ▲ Harrisson et al. [2]; △ Kristmann [6]; + Yamaguchi and Takagi [22]; □ new data. Regression line based on new data only is wt % MgO (ferrite) = 2.0 MgO (bulk) + 0.64.

Ghose and Barnes [5a, 5b] found that in clinkers having widely varying A/F, the alite and belite A/F varied correspondingly. For these oilwell clinkers, with a much more restricted range of A/F, the alite and belite A/F cluster around 1.0 and there is no evidence of a significant correlation with the bulk A/F for either silicate. The alite Al levels are surprisingly high in view of the very low bulk Al content. The positive correlation (Table 3) between Al and Fe contents suggests that the alite Al level follows the high Fe level established by the high bulk Fe. This may be driven by the charge-balance requirement.

Belite

The only two elements for which correlations between belite guest ion level and bulk concentration are statistically significant are Mg and S. However, the Mg contents are very low and the mean is close to zero. Mg substitution in belite is not therefore of any mineralogical significance. The S content, which is variable and much higher, is well estimated by the regression equation

$$\text{wt \% } SO_3\ (belite) = 3.36\ SO_3\ (bulk, \text{corrected for estimated soluble sulphates}) + 0.55.$$

Alternatively, and just as well,

$$\text{wt \% } SO_3\ (belite) = 1.23\ SO_3\ bulk, \text{uncorrected} + 0.24.$$

The mean Al and Fe contents of the belite do not correlate significantly with the bulk clinker Al and Fe contents. However, the ratio A/F is highly correlated (r = 0.93) with the bulk A/F, so that the factors that favor the incorporation of these two impurity ions apparently act similarly on both. This observation agrees qualitatively with the recent data of Fukuda et al. [19], although we find that the belite A/F is somewhat higher than the bulk value, rather than lower. The regression equation is

$$A/F\ (belite) = 1.20\ A/F\ (bulk) + 0.03$$

for the set of nine clinkers.

Ferrite

Our new data confirm that the ferrite MgO content follows closely the bulk MgO. Analyses from several sources are shown together in Figure 4. Our new data and our previous data are almost indistinguishable and in good agreement with most others. Only Ghose and

TABLE 13. Comparison of amounts of clinker phases calculated from modified Bogue calculation and from X-ray compositions of individual phases (see text)

	Alite		Belite		Ferrite		Aluminate	
	mB	X-ray	mB	X-ray	mB	X-ray	mB	X-ray
D1	69.3	67.0	8.5	15.5	19.2	17.2	0	—
D2	68.7	65.6	15.7	15.2	13.9	13.3	0	—
D3	69.4	65.1	16.4	21.8	12.2	12.9	0	—
D4	70.0	75.1	11.0	4.5	16.9	17.5	0.3	2.7
D5	65.3	65.6	17.1	19.3	14.7	14.6	0	—
D6	67.5	73.5	14.1	10.7	16.3	15.7	0	—
D7	62.3	61.8	20.2	22.8	15.5	15.1	0	—
D8	55.6	52.7	29.0	32.1	13.1	13.4	0	1.5
D9	66.4	68.2	14.7	14.1	17.3	17.4	0	—

The modified Bogue (mB) calculation follows closely that of Taylor [14]. There are minor differences in the assumed MgO and TiO_2 contents of the ferrite phase. Columns labelled X-ray give the results of an unweighted least-squares solution of the equation b = Cp (see text).

Barnes [5a, 5b] reported somewhat lower ferrite MgO at corresponding bulk concentrations. The least squares regression equation based on our new data is

$$\text{wt \% } MgO\ (ferrite) = 2.0\ MgO\ (bulk) + 0.64.$$

The evidence for an upper limit is inconclusive. In Figure 4, ferrite MgO and bulk MgO are linearly related to the highest concentrations. The highest ferrite MgO concentrations reported here and elsewhere appear to be approximately 5 wt %, corresponding to approximately 2.3 wt % bulk. This bulk concentration is about that at which cement microscopists report the appearance of free periclase [7,20]. In an unpublished study by Schlumberger of 76 oilwell cements collected worldwide, the bulk MgO content was very variable and often above this: the range was 0.52 to 4.51 wt % (mean 1.23 ± 0.87 SD). Unfortunately, there are no materials in the microanalytical suite with sufficiently high MgO contents for us to be entirely confident about an upper limit to Mg substitution.

Phase Composition

Since we have experimental data both on the composition of the individual clinker phases and on bulk composition, it is possible to estimate the phase assembly. Thus, for each clinker we have a 3×10 composition matrix C, comprising the mean oxide compositions of each clinker mineral by EDS X-ray microanalysis, and a vector b of bulk oxide data by XRF. We seek the solution to the equation $b = Cp$, where $p = [f_1\ f_2\ f_3]$ and f_i are the mass fractions of alite, belite, and ferrite, respectively, in the clinker. With 10 elements common to the X-ray microanalysis and the bulk oxide analysis, the problem is overdetermined and a least-squares solution can be obtained. Both the bulk oxide analysis and the X-ray phase analyses are individually accurate and the main source of error lies in the sampling statistics, since the X-ray microanalytical data are not necessarily representative of the bulk sample.

For two clinkers, D4 and D8, SEM backscattered images showed clear evidence of a separate aluminate phase in the interstitial material. To refine the calculation of the phase assembly for these two clinkers only, the mean X-ray aluminate compositions were included as a fourth component mineral.

Modified Bogue Calculation

These estimated phase assemblies can be compared with the results of calculations made directly from the oxide data alone, using the modified Bogue method described by Taylor [14]. The results are given in Table 13 (see footnote for minor differences between our calculation method and that of Taylor). In four cases, D3, D5, D7, and D8, there is close agreement between the amounts of the four clinker phases calculated from the X-ray data and that computed by the modified Bogue method. In all cases the ferrite is well predicted. However, little confidence can apparently be placed in the computed amounts of alite and belite. This is attributable to the inherent sensitivity of the computed alite/belite ratio to the assumed Ca concentration, particularly in the alite. In the modified Bogue calculation, the total Ca (by XRF) is corrected for soluble sulphate and free lime. One case where this arises is D4: the bulk analysis shows little SO_3 and consequently the Ca adjustment for soluble sulphate is small. However, the X-ray microanalysis does not show especially low SO_3. The inconsistency probably arises from sampling error.

The data suggest that several adjustments to the model phase compositions and some of the rules for calculating them may be justified, at least for oilwell cements having low A/F, such as $A/F < 1$. By comparing the observed clinker mineral compositions and those assumed in the modified Bogue calculation, we conclude that (1) belite MgO is invariably very low and may be assumed to be zero; (2) alite Al_2O_3 is in the range of 1 to 1.5%, rather than 1%, as assumed; (3) belite Al_2O_3 is in the range of 1 to 2%, lower than 2.1%, as assumed; (4) belite Fe_2O_3 is higher (range 1.4 to 2.0%) than assumed (0.9%); (5) alite SO_3 lies in the range of 0.1 to 0.5%, rather than 0; (6) belite SO_3 is much higher than assumed, lying between 0.3 and 1.7%; and (7) ferrite SO_3 is also higher than assumed, in the range of 0 to 0.9%.

Our results suggest that the scheme for estimating the sulphate subsystem is not yet satisfactory. Further study of the distribution of the sulphate ion between the various mineral phases is needed. In most cases, SO_3 is partitioned between at least five minerals. The rules stated by Taylor [14] and based on the work of Pollitt and Brown [21] apparently underestimate the amount of SO_3 in the silicate and ferrite minerals, at least in this class of cement. However, little is known about how the minor sulphate minerals such as aphthitalite, calcium langbeinite, and anhydrite are physically distributed in the clinker microstructure. Until it becomes clearer where and in what form these minerals crystallize, we cannot exclude the possibility that EDS microanalyses of some of the major clinker phases contain contributions from these minor sulphate minerals. For example, the high S contents of the belites, which we find could arise from intimately mixed sulphate minerals, dispersed perhaps in the interlamellar boundaries.

Conclusions

From our observations, we conclude that (1) silicate mineral compositions in oilwell cements are generally similar to those of other portland cements; (2) aluminate is usually absent or present only in very small quantities; (3)

ferrite is very variable and is heavily substituted; and (4) refined phase calculation based on Taylor's modified Bogue method, while generally a good estimator of the phase composition, does not reliably predict alite/belite ratios. It can probably be improved appreciably by minor changes to rules for the composition of individual phases.

Acknowledgment

We thank several cement manufacturers for the supply of production materials and chemical analyses. The X-ray microanalytical data were obtained by Stephen Laing.

References

1. Taylor, H.F.W. *Cement Chemistry*; Academic Press: London, 1990.
2. Harrisson, A.M.; Taylor, H.F.W.; Winter, N.B. *Cem. Concr. Res.* **1985,** *15*, 775–780.
3. Moranville-Regourd, M.; Boikova, A.I. *Ninth International Congress on the Chemistry of Cement*; New Delhi, 1992, Vol. 1, pp 3–45.
4. Ghose, A. PhD thesis, University of London, 1980.

5a. Ghose, A.; Barnes, P. *World Cement Technology* **1980,** *11*, 441–443.

5b. Ghose, A.; Barnes, P. *Cem. Concr. Res.* **1979,** *9*, 745–755.

6. Kristmann, M. *Cem. Concr. Res.* **1978,** *8*, 93–102.
7. Odler, I.; Abdul-Maula, S.; Nüdling, P.; Richter, T. *Zement-Kalk-Gips* **1981,** *34*, 445–449.
8. Bergstrom, T.B.; Hall, C.; Scrivener, K.L. *Adv. Cem. Res.* **1992,** *4*, 141–147.
9. Skibsted, J.; Jakobsen, H.J.; Hall, C. *Journal of the Chemical Society: Faraday Transactions* **1994,** *90*, 2095–2098.
10. Midgley, H.G.; Fletcher, K.E. *Trans. Br. Ceram. Soc.* **1963,** *62*, 917–937.
11. Hahn, T.; Eysel, W.; Woermann, E. *Proceedings of the 5th International Symposium on the Chemistry of Cement*; Tokyo, 1968, Part I, Vol. 1, 61–66.
12. Gies, A.; Knofel, D. *Cem. Concr. Res.* **1987,** *17*, 317–328.
13. Richardson, I.G.; Hall, C.; Groves, G.W. *Adv. Cem. Res.* **1993,** *5*, 15–21.
14. Taylor, H.F.W. *Adv. Cem. Res.* **1989,** *2*, 73–77.
15. Takéuchi, Y.; Nishi, F.; Maki, I. *Zeitschrift für Kristallographie* **1980,** *152*, 259–307.
16. Han, K.S.; Gard, J.A.; Glasser, F.P. *Cem. Concr. Res.* **1981,** *11*, 79–84.
17. Fletcher, K.E. *Mag. Concr. Res.* **1969,** *21*, 3–14.
18. Maki, I.; Fukuda, K.; Yoshida, H.; Kumaki, J. *J. Am. Ceram. Soc.* **1992,** *75*, 3163–3165.
19. Fukuda, K.; Maki, I.; Ito, S.; Yoshida, H.; Kato, C. *J. Am. Ceram. Soc.* **1994,** *77*, 3027–3029.
20. Campbell, D.H. *Microscopical Examination and Interpretation of Portland Cement Clinker*; Construction Technology Laboratories: Skokie, IL, 1986.
21. Pollitt, H.W.W.; Brown, A.W. *Fifth International Symposium on the Chemistry of Cement*; Tokyo, 1968, Vol. 1, pp 322–333.
22. Yamaguchi, G.; Takagi, S. *Fifth International Symposium on the Chemistry of Cement*; Tokyo 1968, pp 181–225.